(14) T. C. Farrar and E. D. Becker, "Pulse and Fourier Transform NMR", Academic Press, New York, 1971, p 20.
(15) J. T. Gerig, G. B. Matson, and A. D. Stock, *J. Magn. Reson.*, **15**, 382 (1974).
(16) S. J. Opella, D. J. Nelson, and O. Jardetsky, *J. Chem. Phys.*, **64**, 2533 (1976).
(17) J. T. Gerig, *J. Am. Chem. Soc.*, **99**, 1721 (1977).
(18) D. W. Scott, D. R. Douslin, J. F. Messerly, S. S. Todd, I. A. Hossenlopp, T. C. Kincheloe, and J. P. McCullough, *J. Am. Chem. Soc.*, **81**, 1015 (1959). A structure of benzotrifluoride in a nematic solvent has been reported: J. Degelan, P. Diehl, and W. Niederberger, *Org. Magn. Reson.*, **4**, 721–723 (1972).
(19) L. J. Berliner and S. S. Wong, *J. Biol. Chem.*, **249**, 1668 (1974).
(20) L. J. Berliner and B. H. Landis in "Nuclear Magnetic Resonance in Molecular Biology," B. Pullman, Ed., D. Reidel Publishing Co., Dordrecht, Holland, 1978, pp 311–322.
(21) A. Kalk and H. J. C. Berendsen, *J. Magn. Reson.*, **24**, 343 (1976).
(22) L. G. Werbelow and A. G. Marshall, *J. Magn. Reson.*, **11**, 299 (1973).
(23) G. B. Matson, *J. Chem. Phys.*, **65**, 4147 (1976).
(24) J. H. Noggle and R. E. Schirmer, "The Nuclear Overhauser Effect", Academic Press, New York, 1971, p 45.
(25) I. Solomon, *Phys. Rev.*, **99**, 559 (1955).
(26) D. E. Woessner, *J. Chem. Phys.*, **36**, 1 (1962).
(27) R. Rowan III, J. A. McCammon, and B. D. Sykes, *J. Am. Chem. Soc.*, **96**, 4773 (1974).
(28) W. E. Hull and B. D. Sykes, *J. Mol. Biol.*, **98**, 121 (1975).
(29) (a) M. W. Pandit and M. S. Narasinga Rao, *Biochemistry*, **14**, 4106–4110 (1975); (b) M. J. Gilleland and M. L. Bender, *J. Biol. Chem.*, **251**, 498–502 (1976); (c) R. Tellam and D. J. Winzor, *Biochem. J.*, **161**, 687–694 (1977).
(30) T. A. Horbett and D. C. Teller, *Biochemistry*, **12**, 1349 (1973).
(31) (a) K. E. Neet and S. E. Brydon, *Arch. Biochem. Biophys.*, **136**, 223 (1970); (b) K. E. Neet, K. M. Sackrison, G. R. Ainslie, and L. C. Barritt, *ibid.*, **160**, 569 (1974).
(32) A. N. Kuznetsov, B. Ebert, and G. V. Gyul Khandanyan, *Mol. Biol. (Moscow)*, **9**, 871 (1975).
(33) W. L. C. Vaz and G. Schoellmann, *Biochim. Biophys. Acta*, **439**, 206 (1976).
(34) A. Gierer and K. Wirtz, *Z. Naturforsch. A*, **8**, 532 (1953).
(35) R. C. Weast, "Handbook of Chemistry and Physics", Vol. 50, Chemical Rubber Publishing Co., Cleveland, Ohio, p F-4.
(36) E. S. Gould, "Mechanism and Structure in Organic Chemistry", Holt, Rinehart and Winston, New York, 1959, p. 51.
(37) (a) K. Wüthrich and G. Wagner, *Trends Biochem. Sci.*, **3**, 227–230 (1978); (b) I. D. Campbell, C. M. Dobson, G. R. Moore, S. J. Perkins, and R. J. P. Williams, *FEBS Lett.*, **70**, 96–100 (1976).
(38) Reference 24, p 28.
(39) (a) J. E. Anderson and W. P. Slichter, *J. Chem. Phys.*, **43**, 433 1965); (b) A. M. I. Ahmed and R. G. Eades, *J. Chem. Soc., Faraday Trans. 2*, 1623 (1972).
(40) T. E. Bull and J. Jonas, *J. Chem. Phys.*, **52**, 1978–1983 (1970).
(41) J. Angerer and W. Suchanski, *J. Magn. Reson.*, **21**, 57–65 (1976).
(42) T. E. Burke and S. I. Chan, *J. Magn. Reson.*, **2**, 120 (1970).
(43) B. R. Appleman and B. P. Dailey, *Adv. Magn. Reson.*, 7, 272 (1974).
(44) L. G. Werbelow and D. M. Grant, *Adv. Magn. Reson.*, **9**, 190–301 (1977).
(45) L. G. Werbelow, *J. Magn. Reson.*, **34**, 123–127 (1979).
(46) H. Jensen and K. Schaumburg, *Mol. Phys.*, **22**, 1041 (1971).
(47) J. B. Lambert and L. G. Greifenstein, *J. Am. Chem. Soc.*, **95**, 6150 (1973).
(48) (a) I. B. Golovanov, V. N. Gazleov, I. A. Soboleva, and V. V. Smolyaninov, *J. Gen. Chem. USSR (Engl. Transl.)*, **43**, 905 (1973); (b) B. Kaufman, M.S. Thesis, State University of New York, Stony Brook, 1972.
(49) W. E. Hull and B. D. Sykes, *Biochemistry*, **15**, 1535 (1976).
(50) J. L. Lippert, D. Tyminski, and P. J. Desmeules, *J. Am. Chem. Soc.*, **98**, 7075 (1976).

Insertion of Tetrafluoroethylene into the Fe–Fe Bond of $(\mu(SCH_3)Fe(CO)_3)_2$, Its Thermal Rearrangement to a Bridging Carbene Ligand, and the Transformation of the Carbene to a Perfluoromethylcarbyne Ligand. Structures of $\mu(SCH_3)_2\mu(C_2F_4)Fe_2(CO)_6$ and $\mu(SCH_3)_2\mu(FCCF_3)Fe_2(CO)_6$ at −162 °C

J. J. Bonnet,[1a] R. Mathieu,[1a] R. Poilblanc,*[1a] and James A. Ibers*[1b]

Contribution from the Laboratoire de Chimie de Coordination, B.P. 4142, 31030 Toulouse-Cedex, France, and the Department of Chemistry, Northwestern University, Evanston, Illinois 60201. *Received March 23, 1979*

Abstract: The insertion of tetrafluoroethylene into the Fe–Fe bond of the dinuclear complex $(\mu(SCH_3)Fe(CO)_3)_2$ is photochemically induced. When the temperature of the reaction is stabilized at 20 °C, the major product is the yellow dinuclear species $\mu(SCH_3)_2\mu(C_2F_4)Fe_2(CO)_6$ (**1**), where C_2F_4 bridges the Fe atoms with two σ(C–Fe) bonds, the C–C bond being parallel to the Fe–Fe axis. When the temperature is higher, i.e., 35 °C, the product is the red dinuclear species $\mu(SCH_3)_2\mu(FCCF_3)Fe_2(CO)_6$ (**2**), which contains a $>CF-CF_3$ carbene bridge. It is possible by heating **1** to obtain **2** and a mechanism for this reaction is proposed, based in part on a study of the action of BF_3 on **1**. The action of BF_3 on **2**, followed by the addition of trimethylphosphine, affords $[\mu(SCH_3)_2Fe_2(CO)_3(PCH_3)_3)_2(CCF_3)][BF_4]$ (**7**), which may be a perfluoromethylcarbyne complex. A proof for the two different kinds of insertion of C_2F_4 is presented in the form of crystal structure determinations of **1** and **2**. In **1** each iron atom is octahedrally coordinated to three carbonyl groups, two bridging S atoms, and one C atom of C_2F_4. The Fe–Fe separation is 3.311 (1) Å, the dihedral angle around the S atoms is 135.0°, and the average Fe–S–Fe angle is 91.6°. Compound **1** crystallizes in the orthorhombic space group D_{2h}^{15}-*Pbca* in a cell of a = 15.029 (8), b = 13.561 (5), c = 15.437 (8) Å. Compound **2** crystallizes with eight formula units in space group C_{2h}^{5}-$P2_1/c$ of the monoclinic system in a cell of dimensions a = 11.545 (3), b = 16.681 (5), c = 16.830 (6) Å with β = 97.86 (2)°. Based on 2471 and 4416 unique reflections for **1** and **2**, respectively, the structures were refined by full-matrix least-squares techniques to conventional agreement indices (on F) of R = 0.044 and R_w = 0.049 for **1** and R = 0.039 and R_w = 0.048 for **2**. In **2**, each iron atom is also octahedrally coordinated, being bound as in **1** to three carbonyl groups, two bridging S atoms, but here to the same bridging C atom of the $>CF-CF_3$ carbene group. The Fe–Fe separation averages 2.963 Å, the dihedral angle around the sulfur atoms is 107.2°, and the average Fe–S–Fe angle is 79.39°. The Fe_2S_2 unit is more compact in **2** than in **1** but less compact than in the starting material $(\mu(SCH_3)Fe(CO)_3)_2$. The flexibility of such molecules around the S–S axis, together with the reactivity of the Fe–Fe bond, is discussed.

The study of the reactivity of the metal–metal bond in dinuclear complexes toward alkynes, alkenes, or more generally small unsaturated molecules is an increasing field of interest. This is particularly true for dinuclear complexes with metal to metal multiple bonds.[2,3] However, insertion reactions of alkynes and alkenes into metal–metal single bonds in dinuclear

0002-7863/79/1501-7487$01.00/0

Table I. Summary of Crystal Data and Intensity Collection

compd	$\mu(SCH_3)_2\mu(C_2F_4)Fe_2(CO)_6$ (**1**)	$\mu(SCH_3)_2\mu(FCCF_3)Fe_2(CO)_6$ (**2**)
formula	$C_{10}H_6F_4Fe_2O_6S_2$	$C_{10}H_6F_4Fe_2O_6S_2$
formula weight	473.97 amu	473.97 amu
a (at −162 °C)	15.029 (8) Å	11.545 (3) Å
b	13.561 (5) Å	16.681 (3) Å
c	15.437 (8) Å	16.830 (6) Å
β		97.86 (1)°
V	3146 Å^3	3211 Å^3
Z	8	8
density (calcd, −162 °C	2.00 g cm^{-3}	1.96 g cm^{-3}
density (measured (20 °C) in aqueous $ZnCl_2$)	1.90 g cm^{-3}	1.85 g cm^{-3}
space group	D_{2h}^{15}-*Pbca*	C_{2h}^5-$P2_1/c$
crystal dimensions	0.175 × 0.092 × 0.278 mm	0.146 × 0.252 × 0.219 mm
boundary faces of the prism	{001}, (210), ($\bar{2}\bar{1}0$), (2$\bar{1}$0), (210)	{100}, {011}
crystal volume	0.0425 mm^3	0.0784 mm^3
temp	−162 °C[a]	−162 °C
radiation	Mo Kα from monochromator (λ(Mo Kα$_1$) = 0.709 30 Å)	Mo Kα from monochromator
linear absorption coefficient	21.7 cm^{-1}	21.2 cm^{-1}
transmission factors	0.433–0.708	0.640–0.763
receiving aperture	4.0 × 4.0 mm; 30 cm from crystal	4.0 × 4.5 mm; 30 cm from crystal
take-off angle	3.2°	2.6°
scan speed	2° in 2θ/min	2° in 2θ/min
scan range	0.7° below Kα$_1$ to 0.7° above Kα$_2$	0.6° below Kα$_1$ to 0.6° above Kα$_2$
background counts	10 s with rescan option[b]	10 s with rescan option
2θ limits	2.5–56°	2.5–50°
final no. of variables	254	433
unique data used	2471 $F_o^2 > 3\sigma(F_o^2)$	4416 $F_o^2 > 3\sigma(F_o^2)$
$R = \Sigma\|\|F_o\| - \|F_c\|\|/\Sigma\|F_o\|$	0.044	0.039
$R_w = (\Sigma w(\|F_o\| - \|F_c\|)^2/\Sigma wF_o^2)^{1/2}$	0.049	0.048
standard error in an observation of unit weight	1.22 e	1.29 e

[a] The low-temperature system is based on a design by J. C. Huffman, Ph.D. Thesis, Indiana University, 1974. [b] The diffractometer was run under the Vanderbilt disk oriented system (Lenhert, P.G. *J. Appl. Crystallogr.* **1975**, *8*, 568).

complexes are less studied.[4-6] Furthermore, although the discovery of the first transition-metal carbene was reported 15 years ago,[7] little is known about carbenes bound to two metal centers.[8-12]

We have shown recently[13] that with photochemical activation it is possible to insert the alkynes $F_3CC{\equiv}CCF_3$ or $H_3COOCC{\equiv}CCOOCH_3$ into the Fe—Fe bond of $(\mu(SR)Fe(CO)_3)_2$ complexes (R = CH_3 and C_6H_5). We have now extended this study to the insertion of C_2F_4. We find that not only does C_2F_4 insert directly into the Fe-Fe bond, but it rearranges thermally to a bridging carbene ligand which can be transformed to a perfluoromethylcarbyne ligand. The results of these investigations are presented here.

Experimental Section

All reactions were carried out under a pure dinitrogen atmosphere using Schlenk tubes and vacuum line procedures. Infrared spectra (hexadecane solutions) were recorded on a Perkin-Elmer 225 spectrometer. ^{1}H NMR spectra were recorded on a Varian A-60A spectrometer and ^{19}F NMR spectra on a Perkin-Elmer R 10 spectrometer (dichloromethane solutions). Elemental analyses were performed by the Service Central de Microanalyse du CNRS. The starting material $(\mu(SCH_3)Fe(CO)_3)_2$ was purchased from Pressure Chemical Co. and C_2F_4 was generated by pyrolysis of Teflon under vacuum.

Preparation of $\mu(SCH_3)_2\mu(C_2F_4)Fe_2(CO)_6$ (1). $(\mu(SCH_3)Fe(CO)_3)_2$ (0.5 g) was dissolved in benzene and introduced into a vessel fitted with a Teflon stopcock. From a vacuum line a tenfold excess of C_2F_4 was condensed into the vessel. The stirred solution was then irradiated at 20 °C for 16 h using a water-cooled 150-W Original Hanau TQ 150 mercury vapor lamp placed approximately 10 cm from the vessel. At the end of the reaction the benzene was evaporated to dryness, the residue was dissolved in a small amount of toluene and filtered, and then an equal amount of pentane was added. The solution was then cooled to −20 °C. Yellow parallelepipeds were obtained (0.210 g, 33% yield), mp 93 °C dec. Anal. Calcd for $C_{10}H_6F_4Fe_2O_6S_2$: C, 25.31; H, 1.26; F, 16.03. Found: C, 25.27; H, 1.33; F, 15.64. IR: ν(CO) 2100 vw, 2084 vs, 2040 s, 2033 s cm^{-1}. ^{1}H NMR (CH_2Cl_2): δ 2.36 (SCH_3, s), 1.86 ppm (SCH_3, s). ^{19}F NMR (CH_2Cl_2), CCl_3F as reference, AB spin system: δ_A 56.4, δ_B 61.9 ppm; J_{AB} = 227 Hz.

Preparation of $\mu(SCH_3)_2\mu(FCCF_3)Fe_2(CO)_6$ (2). This compound was prepared in the same way as **1** except that the solution was irradiated at 35 °C using a 500-W Original Hanau TQ 718 water-cooled mercury vapor lamp. Evaporation of the solvent gave a green product, **3** (vide infra). Pentane was then added and CO was bubbled through the solution. The red compound **2** was regenerated along with some amount of the starting compound $(\mu(SCH_3)Fe(CO)_3)_2$. The pentane solution was filtered and cooled to −20 °C. Red, air-stable crystals of **2** were obtained (0.250 g, 40% yield), mp 80 °C. Anal. Calcd for $C_{10}H_6F_4Fe_2O_6S_2$: C, 25.31; H, 1.26; F, 16.03. Found: C, 25.39; H, 1.29; F, 16.03. IR: ν(CO) 2095 w, 2091 vw, 2074 vs, 2069 m (sh), 2027 s (broad), 2021 sh cm^{-1}. ^{1}H NMR: δ 2.17, 2.07 (SCH_3 anti isomer); 2.15 ppm broad, SCH_3 (syn isomer). ^{19}F NMR: δ 70 (3 F) (q), 138 ppm (1 F) (q), J_{FF} = 7 Hz (syn isomer); δ 68.8 (3 F) (d), 136.8 ppm (1 F) (q), J_{FF} = 7 Hz (anti isomer).

Isolation of the Green Compound 3. In the above preparation of **2**, after evaporation of benzene, the green precipitate was washed with pentane and dried. The product was then dissolved in a minimum amount of CH_2Cl_2 and immediately precipitated by adding a small amount of pentane. Anal. Calcd for $[(\mu(SCH_3)Fe(CO)_2]_3(C_2F_4)]_n$: C, 22.87; H, 1.55; F, 13.17. Found: C, 22.49; H, 1.48; F, 12.77.

Preparation of $\mu(SCH_3)_2\mu(C_2F_4)Fe_2(CO)_4(P(CH_3)_3)_2$ (4) and $\mu(SCH_3)_2\mu(FCCF_3)Fe_2(CO)_4(P(CH_3)_3)_2$ (5). To a solution of **1** or **2** in pentane was added at room temperature a stoichiometric quantity of $P(CH_3)_3$. Gaseous CO was evolved and respectively **4** or **5** precipitated as yellow (**4**) or dark red (**5**) crystals. They were purified by recrystallization from a CH_2Cl_2/pentane mixture at −20 °C, yield 90%. $\mu(SCH_3)_2\mu(C_2F_4)Fe_2(CO)_4(P(CH_3)_3)_2$ (**4**), mp 150 °C dec. Anal. Calcd for $C_{14}H_{24}F_4Fe_2O_4P_2S_2$: C, 29.47; H, 4.21; P, 10.87; F, 13.33. Found: C, 29.50; H, 4.18; P, 10.79; F, 13.43. IR ν(CO): 2027 w, 2013 s, 1965 s cm^{-1} (CH_2Cl_2 solution). ^{1}H NMR: δ 1.86 (SCH_3), 1.45 ppm, J_{PH} = 8 Hz ($P(CH_3)_3$). ^{19}F NMR: δ 49.4 ppm (broad signal). $\mu(SCH_3)\mu(FCCF_3)Fe_2(CO)_4(P(CH_3)_3)_2$ (**5**) mp 140 °C dec. Anal.

Table II. Positional and Thermal Parameters for the Atoms of $\mu(SCH_3)_2\mu(C_2F_4)Fe_2(CO)_6$ (**1**)

ATOM	X[A]	Y	Z	B11 OR B,A^2	B22	B33	B12	B13	B23
FE(1)	0.454005(45)	0.247543(51)	0.466341(46)	13.48(29)	16.90(33)	11.47(29)	2.05(30)	-0.65(26)	-0.71(27)
FE(2)	0.313861(48)	0.415425(48)	0.391197(45)	16.78(33)	16.10(35)	10.17(30)	0.44(29)	-3.34(27)	1.57(27)
S(1)	0.317850(79)	0.318548(85)	0.508689(75)	12.74(51)	18.04(58)	9.81(48)	-0.26(46)	0.40(43)	0.80(42)
S(2)	0.466050(81)	0.404742(84)	0.409998(78)	15.67(54)	19.45(62)	8.12(47)	-2.13(47)	0.44(42)	-1.31(44)
F(1)	0.35801(60)	0.11591(58)	0.35096(58)	25.3(45)	23.6(38)	25.6(40)	5.1(31)	-13.7(30)	-5.5(29)
F(2)	0.44513(48)	0.21671(73)	0.28341(47)	20.9(31)	47.3(53)	15.2(28)	-3.8(34)	5.0(24)	-16.2(33)
F(3)	0.23294(48)	0.23018(43)	0.35373(59)	16.7(30)	28.3(38)	40.4(47)	-6.6(24)	-1.7(27)	-11.2(30)
F(4)	0.38193(58)	0.28973(50)	0.24300(40)	53.9(68)	49.6(43)	11.9(26)	24.4(45)	-14.8(32)	-12.8(28)
F(1)*	0.32495(75)	0.13441)76)	0.38011(74)	30.9(55)	20.2(51)	32.6(52)	-16.5(42)	-8.6(39)	7.8(39)
F(2)*	0.43611(64)	0.16218(85)	0.29705(55)	29.6(43)	48.3(60)	11.3(34)	20.3(44)	-3.9(29)	-17.2(39)
F(3)*	0.25016(51)	0.25327(56)	0.29064(65)	23.7(35)	28.2(40)	45.0(68)	5.4(35)	-20.3(44)	-14.4(43)
F(4)*	0.37373(75)	0.31235(58)	0.23901(44)	58.9(67)	28.4(39)	8.4(30)	-0.2(37)	4.9(31)	-4.2(26)
O(1)	0.62129(25)	0.18281(31)	0.38656(28)	16.8(18)	54.1)27)	37.1(23)	10.7(18)	0.9(17)	-16.5(20)
O(2)	0.54556(25)	0.31893(28)	0.62617(23)	24.9(19)	37.5(23)	15.8(16)	-0.5)18)	-7.3(15)	-2.0(16)
O(3)	0.40913(29)	0.05466(26)	0.54217(27)	42.3(23)	24.5(21)	28.1(21)	2.3)18)	-1.7(18)	6.3(17)
O(4)	0.33188(30)	0.52453(33)	0.22858(27)	40.2)24)	66.8(30)	20.7(19)	2.4(22)	-6.3(18)	23.0(20)
O(5)	0.31527(24)	0.59488(26)	0.50303(24)	24.4(19)	23.1(21)	25.0(18)	2.3(16)	-2.2(16)	-5.3(16)
O(6)	0.11856(26)	0.40413(27)	0.38582(26)	23.2(20)	35.1(24)	29.9(22)	-2.6(17)	-8.1(16)	2.7(18)
C(1)	0.55662(35)	0.20624(38)	0.41801(36)	17.6(26)	27.2(28)	19.6(25)	1.7(21)	-7.4(20)	-5.8(22)
C(2)	0.51179(34)	0.29139(37)	0.56563(34)	14.4(23)	26.8(27)	16.2(24)	2.7(21)	2.9(19)	1.9(21)
C(3)	0.42770(36)	0.12888(39)	0.51224(35)	21.2(26)	21.6(27)	20.5(25)	2.6(21)	-5.1(20)	-0.6(21)
C(4)	0.32421(37)	0.48350(39)	0.29165(36)	22.6(27)	34.6(30)	20.3(26)	6.3(23)	-1.4(22)	4.9(22)
C(5)	0.31489(34)	0.52801(35)	0.45978(35)	15.0(23)	20.6(26)	20.1(24)	1.2(20)	2.3(20)	3.5(21)
C(6)	0.19420(37)	0.40987(35)	0.38697(34)	22.8(27)	18.4(25)	16.6(22)	0.7(21)	-5.4(20)	1.3(20)
C(7)	0.33578(35)	0.38539(37)	0.60469(32)	19.6(24)	28.4(28)	10.6(20)	4.2(21)	3.8)18)	-4.4(19)
C(8)	0.52784(37)	0.40934(42)	0.30817(33)	32.1(28)	39.9(34)	14.6(21)	-14.3(26)	11.4(20)	-3.2)23)
C(9)	0.38615(35)	0.21074(36)	0.35709(33)	18.2(24)	21.1(25)	13.1(22)	-1.1)21)	0.2(18)	-5.8(19)
C(10)	0.31793(45)	0.28689(40)	0.32575(39)	46.2(36)	29.1(30)	26.0(28)	9.0(28)	-23.3(27)	-10.9(24)
H1C(7)	0.328	0.346	0.656	2.6					
H2C(7)	0.395	0.411	0.605	2.6					
H3C(7)	0.295	0.439	0.606	2.6					
H1C(8)	0.590	0.412	0.319	3.2					
H2C(8)	0.515	0.351	0.274	3.2					
H3C(8)	0.510	0.466	0.275	3.2					

[a] Estimated standard deviations in the least significant figure(s) are given in parentheses in this and all subsequent tables. [b] The form of the anisotropic thermal ellipsoid is $\exp(-(\beta_{11}h^2 + \beta_{22}k^2 + \beta_{33}l^2 + 2\beta_{12}hk + 2\beta_{13}hl + 2\beta_{23}kl))$. Here and in Table IV the thermal coefficients have been multiplied by 10^4.

Calcd for $C_{14}H_{24}F_4Fe_2O_4P_2S_2$: C, 29.47; H, 4.21; P, 10.87; F, 13.33. Found: C, 29.38; H, 4.23; P, 10.52; F, 13.10. IR ν(CO): 2017 w, 1977 s, 1953 s cm^{-1} (CH_2Cl_2 solution). ^1H NMR: δ 1.86 (SCH_3(s)), 2.20 (SCH_3)(d)) J_{FH} = 0.9 Hz, 1.30 ppm PCH_3, J_{PH} = 7.8 Hz. ^{19}F NMR: δ 66.6 (3 F) (broad signal), 130 ppm (1 F) (broad signal).

Preparation of $[\mu(SCH_3)_2Fe_2(CO)_4(P(CH_3)_3)_2(FCCF_2)][BF_4]$ (6). To a yellow solution of **4** in CH_2Cl_2 at 0 °C was added a stoichiometric quantity of $BF_3{\cdot}O(CH_3)_2$. The solution turned violet. Chilled diethyl ether was added (1:1 mixture). The solution was then kept at −20 °C and maroon crystals precipitated. $[\mu(SCH_3)_2Fe_2(CO)_4(P(CH_3)_3)_2(FCCF_2)][BF_4]$, mp 72 °C dec. Anal. Calcd for $C_{14}H_{24}BF_7Fe_2O_4P_2S_2$: C, 26.33; H, 3.76; F, 20.84. Found: C, 26.16; H, 3.71; F, 20.66. IR ν(CO): 2054 w, 2040 s, 2003 s cm^{-1} (CH_2Cl_2 solution), ν(C=C) 1600 cm^{-1}. ^1H NMR: δ 2.81, 2.28 (SCH_3, broad signals), 1.68, J_{PH} = 11 Hz ($P(CH_3)_3$), 1.57 ppm, J_{PH} = 11.5 Hz ($P(CH_3)_3$).

Preparation of $[\mu(SCH_3)_2Fe_2(CO)_3(P(CH_3)_3)_2(CCF_3)][BF_4]$ (7). To a solution of **5** in CH_2Cl_2 was added at room temperature a stoichiometric amount of $BF_3{\cdot}O(CH_3)_2$. The reddish solution turned bright red and diethyl ether was added. Evolution of CO was detected, with 1 mol of CO being evolved per mol of **5**. From the solution at −20 °C dark red crystals precipitated. $[\mu(SCH_3)_2Fe_2(CO)_3(P(CH_3)_3)_2(CCF_3)][BF_4]$, mp 182 °C dec. Anal. Calcd for $C_{13}H_{24}BF_7Fe_2O_3P_2S_2$: C, 25.57; H, 3.93; F, 21.80. Found: C, 25.55; H, 3.72; F, 21.74. IR ν(CO): 2042 vs, 2015 s, 1984 w (CH_2Cl_2 solution). ^1H NMR: δ 2.62 (SCH_3, q) J_{PH} = 2.6 Hz, 2.13 (SCH_3, s), 1.96 ($P(CH_3)_3$) J_{PH} = 10 Hz, 1.65 ppm ($P(CH_3)_3$) J_{PH} = 11 Hz. ^{19}F NMR: δ 78.4 ppm (CF_3, broad signal).

Collection and Reduction of the X-ray Data. A. Compound 1. Preliminary photographic data revealed that crystals of **1** belong to the orthorhombic system and show systematic extinctions ($0kl$, $k = 2n + 1$; $h0l$, $l = 2n + 1$; $hk0$, $h = 2n + 1$) consistent with the space group D_{2h}^{15}-*Pbca*. All cell constants were obtained as previously described[14] by a least-squares refinement of the setting angles of 19 hand-centered reflections which had been chosen from diverse regions of reciprocal space with $24° < 2\theta(Mo) < 26°$. These cell constants and other pertinent data are presented in Table I. Intensity data were collected at −162 °C on a computer-controlled Picker four-circle diffractometer by procedures standard for this laboratory.[15] A total of 4564 intensities were recorded out to $2\theta(Mo) < 56°$. The data were processed, as described previously,[14] using a value of p of 0.04. After processing[16] only those 2471 unique reflections having $F_o^2 > 3\sigma(F_o^2)$ were used in subsequent calculations.

B. Compound 2. Preliminary film data showed that crystals of **2** belong to the monoclinic system and show systematic extinctions ($0k0$, $k = 2n + 1$; $h0l$, $l = 2n + 1$) consistent with the space group C_{2h}^5-$P2_1/c$. Cell constants were obtained by a least-squares refinement of the setting of 22 hand-centered reflections with $23° < 2\theta(Mo) < 26°$. These cell constants and other pertinent data are listed in Table I. Intensity data were collected at −162 °C. A total of 6218 intensities reflections were recorded out to $2\theta(Mo) < 50°$. The data were processed in the normal manner using a value of p of 0.04.[14] Only those 4416 unique reflections having $F_o^2 > 3\sigma(F_o^2)$ were used in subsequent calculations.

Solution and Refinement of the Structures. Complex 1. The two iron atoms together with the two sulfur atoms were located in a normal Patterson synthesis. The positions of the remaining nonhydrogen atoms were obtained through the usual combination of full-matrix least-squares refinements and difference Fourier syntheses. Around the fluorine atoms of the C_2F_4 group eight electron density maxima of height 4–5 e/Å^3 were located on a difference Fourier map. These maxima correspond to two alternative positions for four fluorine atoms. Owing in large measure to the acquisition of low-temperature data, the disorder problem has been resolved, even though the shortest distance between the maxima is about 0.7 Å. During the course of full-matrix, least-squares refinement the positional and thermal pa-

Table IV. Positional and Thermal Parameters for the Atoms of $\mu(SCH_3)_2\mu(FCCF_3)Fe_2(CO)_6$ (2)

ATOM	A X	Y	Z	B B11	B22	B33	B12	B13	B23
FE(1)A	0.028835(52)	0.438347(36)	0.163009(34)	25.80(49)	12.79(23)	9.33(22)	1.16(26)	2.36(25)	0.67(18)
FE(2)A	-0.038332(53)	0.433723(37)	0.326359(36)	24.85(50)	16.57(25)	11.21(23)	3.11(26)	1.75(26)	1.61(19)
FE(1)B	0.426633(54)	0.322190(36)	0.468043(38)	24.98(50)	13.16(24)	15.38(25)	1.90(27)	1.18(27)	2.22(19)
FE(2)B	0.569485(52)	0.205770(37)	0.389919(37)	20.79(47)	13.56(23)	13.56(24)	-0.43(26)	0.61(26)	-0.08(18)
S(1)A	0.118545(91)	0.373918(62)	0.276989(63)	22.37(79)	11.98(38)	13.07(39)	0.22(44)	1.67(44)	1.41(31)
S(2)A	-0.136509(93)	0.384843(68)	0.206418(64)	21.39(82)	18.39(43)	13.50(40)	1.50(48)	3.86(45)	1.28(34)
S(1)B	0.405984(93)	0.277908(68)	0.336125(66)	22.62(83)	17.94(43)	16.40(42)	0.56(48)	-0.59(46)	0.44(34)
S(2)B	0.621432(94)	0.329475(66)	0.447918(66)	26.09(83)	14.67(41)	15.59(41)	1.84(47)	-0.93(46)	-1.57(33)
F(1)A	-0.09425(22)	0.57219(14)	0.22456(15)	35.9(22)	15.16(97)	21.5(10)	6.1(12)	-4.7(12)	1.83(81)
F(2)A	0.19957(22)	0.54452(15)	0.30011(15)	36.0(22)	16.6(10)	22.3(11)	1.5(12)	-3.9(12)	-0.71(83)
F(3)A	0.11554(25)	0.62836(15)	0.21295(17)	64.7(26)	16.8(10)	26.6(12)	-2.5(13)	5.3(14)	5.49(90)
F(4)A	0.06991(25)	0.62758(16)	0.33378(16)	68.5(27)	20.7(11)	23.3(11)	9.5(14)	-10.8(14)	-11.57(90)
F(1)B	0.54324(22)	0.18998(15)	0.55885(15)	40.1(22)	23.0(11)	18.4(10)	4.4(12)	1.3(12)	7.19(84)
F(2)B	0.30024(23)	0.14479(17)	0.41803(17)	42.0(23)	25.2(12)	27.8(12)	-10.8(13)	4.2(14)	1.20(96)
F(3)B	0.31763(24)	0.15568(17)	0.54767(17)	55.5(25)	30.0(12)	30.4(12)	4.3(14)	22.8(14)	11.6(10)
F(4)B	0.41981(26)	0.06783(16)	0.49297(18)	71.5(28)	15.2(10)	38.7(14)	4.8(14)	18.4(16)	6.39(96)
O(1)A	-0.10310(29)	0.54277(20)	0.04386(18)	51.3(30)	29.5(14)	13.1(12)	13.1(17)	2.7(15)	6.6(11)
O(2)A	0.25989(28)	0.49608(20)	0.13511(19)	33.6(27)	24.3(14)	25.2(14)	-6.4(16)	3.4(15)	6.1(11)
O(3)A	0.02780(30)	0.29473(20)	0.05715(20)	54.7(31)	26.7(14)	25.7(14)	2.0(17)	4.2(17)	-16.3(12)
O(4)A	-0.23900(31)	0.52859(23)	0.36154(21)	55.7(33)	44.7(18)	23.2(15)	24.6(21)	7.5(18)	-6.1(13)
O(5)A	0.12114(29)	0.49382(21)	0.46341(19)	47.4(30)	34.4(16)	15.6(13)	3.2(18)	-2.7(16)	-6.3(12)
O(6)A	-0.10051(28)	0.28195(20)	0.40368(20)	36.6(28)	30.7(15)	22.9(14)	-3.8(17)	5.9(15)	13.1(12)
O(1)B	0.47327(32)	0.34529(22)	0.64186(20)	64.2(34)	39.4(17)	15.3(14)	11.3(19)	1.8(17)	-8.3(12)
O(2)B	0.17568(28)	0.30221(20)	0.47232(21)	31.0(29)	30.9(15)	29.2(15)	2.3(16)	6.6(16)	11.8(12)
O(3)B	0.40002(30)	0.49437(20)	0.42283(21)	52.8(32)	15.0(13)	33.5(16)	5.9(16)	-3.4(18)	4.2(12)
O(4)B	0.76924(28)	0.12933(19)	0.48645(19)	40.2(27)	18.2(13)	22.4(13)	9.2(16)	-1.8(16)	8.4(11)
O(5)B	0.47762(30)	0.05601(20)	0.31441(22)	52.0(31)	20.9(14)	36.4(17)	-13.3(17)	3.7(18)	-7.5(13)
O(6)B	0.68702(28)	0.24227(20)	0.24719(20)	36.4(27)	28.3(15)	22.2(14)	-6.1(16)	5.6(16)	-8.6(12)
C(1)A	-0.05199(38)	0.50120(29)	0.08943(26)	31.0(36)	25.1(20)	11.3(16)	-2.3(22)	9.2(20)	-3.4(15)
C(2)A	0.16907(42)	0.47433(26)	0.14497(26)	48.7(42)	14.7(17)	12.0(16)	-0.6(22)	1.3(21)	2.4(13)
C(3)A	0.03141(37)	0.34984(28)	0.09650(26)	24.7(34)	28.8(19)	16.6(17)	-0.9(20)	4.1(19)	2.3(15)
C(4)A	-0.16157(45)	0.49188(31)	0.34902(27)	48.5(44)	30.2(22)	12.0(17)	6.5(26)	-0.3(22)	-2.6(16)
C(5)A	0.05885(40)	0.47040(29)	0.41017(27)	36.2(38)	22.4(19)	15.4(18)	13.0(22)	4.1(22)	-8.8(15)
C(6)A	-0.07735(38)	0.34062(31)	0.37614(27)	24.9(34)	28.3(22)	13.1(17)	5.6(23)	3.1(19)	4.6(16)
C(7)A	0.09191(39)	0.26677(26)	0.26534(29)	35.4(37)	11.3(16)	25.1(19)	-0.9(20)	2.2(21)	1.0(14)
C(8)A	-0.26824(38)	0.44161(28)	0.17371(27)	24.6(35)	21.7(19)	17.5(18)	5.8(21)	-1.1(20)	8.1(15)
C(9)A	0.00303(40)	0.51933(28)	0.24871(27)	34.7(37)	18.1(18)	14.9(17)	5.3(21)	-3.4(20)	8.8(15)
C(10)A	0.09682(42)	0.57878(29)	0.27389(29)	42.7(41)	20.4(19)	21.2(20)	3.2(23)	-0.5(23)	8.6(16)
C(1)B	0.45578(39)	0.33718(29)	0.57403(30)	30.7(37)	21.1(19)	24.7(22)	5.0(21)	4.8(22)	2.5(16)
C(2)B	0.27387(41)	0.30840(26)	0.47040(27)	41.7(42)	17.0(18)	17.0(17)	8.8(21)	3.9(21)	8.2(14)
C(3)B	0.40889(38)	0.42873(29)	0.44029(27)	25.0(36)	21.1(20)	16.6(18)	3.4(21)	0.3(20)	1.3(15)
C(4)B	0.69102(38)	0.15791(26)	0.44842(26)	34.7(36)	10.4(16)	17.0(17)	-1.4(20)	8.3(20)	1.0(14)
C(5)B	0.51153(38)	0.11424(30)	0.34491(28)	23.3(35)	23.4(20)	21.8(19)	1.0(22)	2.8(20)	3.4(16)
C(6)B	0.64504(37)	0.22803(26)	0.30249(28)	24.7(34)	14.9(17)	18.6(18)	1.5(19)	-2.2(20)	-1.5(14)
C(7)B	0.44994(40)	0.35751(29)	0.27353(28)	37.3(38)	24.3(19)	16.9(18)	4.5(22)	1.2(21)	4.6(15)
C(8)B	0.71818(37)	0.31962(28)	0.54237(26)	26.8(34)	21.4(19)	17.1(17)	3.0(21)	-5.2(19)	-6.8(14)
C(9)B	0.47356(38)	0.20415(27)	0.48272(26)	31.4(36)	21.2(18)	13.3(16)	1.7(21)	1.2(19)	3.8(14)
C(10)B	0.37938(43)	0.14353(29)	0.48450(30)	45.2(42)	19.3(19)	25.4(21)	4.4(23)	8.4(24)	4.5(16)
H1C(7)	0.085	0.244	0.316	2.9					
H2C(7)	0.021	0.258	0.230	2.9					
H3C(7)	0.155	0.242	0.244	2.9					
H1C(8)	-0.303	0.458	0.218	3.0					
H2C(8)	-0.248	0.488	0.144	3.0					
H3C(8)	-0.321	0.409	0.139	3.0					
H1C(7)	0.477	0.402	0.306	3.1					
H2C(7)	0.512	0.339	0.246	3.1					
H3C(7)	0.386	0.373	0.235	3.1					
H1C(8)	0.675	0.323	0.587	2.9					
H2C(8)	0.758	0.269	0.545	2.9					
H3C(8)	0.776	0.361	0.548	2.9					

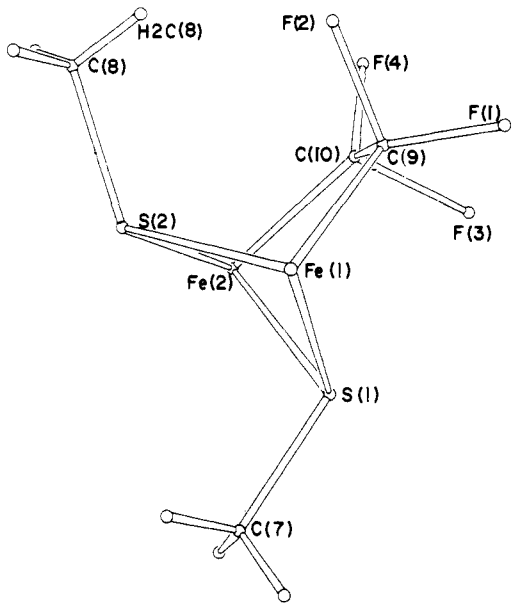

Figure 1. A sketch of the structure of $\mu(SCH_3)_2\mu(C_2F_4)Fe_2(CO)_6$ without the carbonyl groups to show the two different environments for fluorine atoms F(2), F(4) and F(1), F(3).

rameters of the eight fluorine atoms were allowed to vary independently. A variable occupancy factor, α, was assigned to those four fluorine atoms giving almost a staggered geometry, and the occupancy of the other four fluorine atoms was constrained to $1 - \alpha$.

Atomic scattering factors for the nonhydrogen atoms were taken from the usual tabulation,[17] whereas the hydrogen scattering factors used were those of Stewart et al.[18] Anomalous dispersion terms for the Fe and S atoms were included in F_c.[19]

Refinement of an isotropic model converged to values of R and R_w of 0.067 and 0.076. A difference Fourier map clearly revealed the positions of the six H atoms of the two methyl groups. Their positions were idealized (C–H = 0.95 Å). Their contributions to F_c were then fixed during the final cycles of refinement which included an isotropic secondary extinction correction and anisotropic thermal parameters for all but the hydrogen atoms. For each hydrogen atom, an isotopic thermal parameter was assigned with a value 1.0 Å^2 greater than that of the C atom to which it is attached.

The final positional and thermal parameters of all atoms appear in Table II. The occupancy of atoms F(1)–F(4) is 0.54 and that of atoms F(1)′–F(4)′ is 0.46. Table III contains the root-mean-square amplitudes of vibration.[20] A listing of the observed and calculated structure amplitudes is available.[20]

Complex 2. The direct methods approach,[16] based on 499 normalized structure factors, yielded the correct positions of the four Fe and four S atoms belonging to two independent dinuclear molecules in the asymmetric unit. All other atoms, including the hydrogen atoms of the methyl groups, were found in subsequent difference Fourier syntheses. The existence of the $>CFCF_3$ bridge came as a complete surprise.

Refinement of a completely isotropic model for the two independent molecules with no contribution from H atoms converged to values of R of 0.060 and R_w of 0.074. A subsequent difference Fourier map revealed the positions of hydrogen atoms of the methyl groups. These were treated as in **1**. The final full-matrix least-squares refinements, involving 433 variables and 4416 observations, were carried out by remote hookup to the CDC 7600 computer at Lawrence Berkeley Laboratory. Final values of the parameters of all atoms are given in Table IV. The root-mean-square amplitudes of vibration are listed in Table V.[20] A listing of the observed and calculated structure amplitudes is available.[20]

Results

Syntheses and Reactions. When C_2F_4 is added to a benzene solution of $(\mu(SCH_3)Fe(CO)_3)_2$ and irradiation is carried out so that the temperature of the solution is ca. 20 °C, a diamagnetic dinuclear compound, $\mu(SCH_3)_2\mu(C_2F_4)Fe_2(CO)_6$ (**1**), may be obtained from this solution as yellow crystals. The

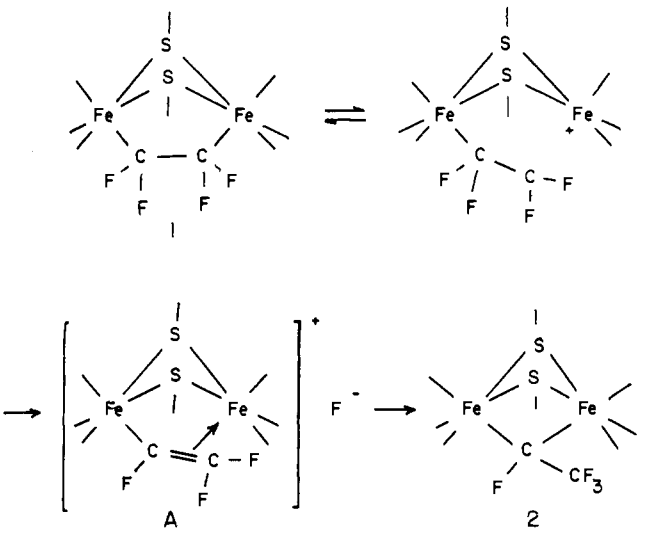

Figure 2. Proposed mechanism of rearrangement of the C_2F_4 bridging group in $\mu(SCH_3)_2\mu(C_2F_4)Fe_2(CO)_6$ to give the $>CF-CF_3$ bridge in $\mu(SCH_3)_2\mu(FCCF_3)Fe_2(CO)_6$.

spectral properties of **1** are completely consistent with its solid-state structure as found by diffraction methods (vide infra). Complex **1** shows an infrared spectrum in the $\nu(CO)$ stretching region which is very similar to that observed for $\mu(SCH_3)_2\mu(F_3CC{\equiv}CCF_3)Fe_2(CO)_6$ in which the alkyne is σ bonded to the two iron atoms.[12] The ^1H NMR spectrum shows clearly that the two SCH_3 groups are in the anti position. The ^{19}F NMR spectrum shows an approximate AB system in a region of resonance for C_2F_4 bridging two metallic centers;[21] this AB spin system is consistent with the fact that since the SCH_3 groups are in the anti position two of the four fluorine atoms are indeed nearer to the SCH_3 group which is in the endo position (Figure 1).

When C_2F_4 is added to a benzene solution of $(\mu(SCH_3)Fe(CO)_3)_2$ and irradiation is carried out so that the temperature of the solution is ca. 35 °C, a different product is obtained. From this red solution a diamagnetic dinuclear complex, $\mu(SCH_3)_2\mu(FCCF_3)Fe_2(CO)_6$ (**2**), is obtained as red crystals. The nature of this product was first established from the solid-state crystal structure (vide infra). The spectral properties of this material are consistent with that formulation. The ^1H NMR spectrum shows that the complex is a mixture of syn and anti isomers in the ratio 2/1. The ^{19}F NMR spectrum shows two sets of signals, a doublet and a quartet, in the ratio 3:1 consistent with a rearrangement of the C_2F_4 group into a carbene bridge $>CF-CF_3$, as in $Co_2(CO)_7(FCCF_3)$.[6]

It is also possible to effect this rearrangement and obtain **2** by heating **1** in refluxing pentane. This transformation even occurs in the infrared beam of the Perkin-Elmer 225 spectrometer. Compound **2** is stable in the solid state but in solution it gives, under vacuum, a green precipitate (**3**). Compound **3** is soluble in acetone or dichloromethane, but the solution is unstable and quickly turns red. The infrared spectrum shows this red solution to be a mixture of $(\mu(SCH_3)Fe(CO)_3)_2$ and **2**. If CO gas is added to a solution of **3**, the same mixture is readily obtained. Furthermore, if $P(CH_3)_3$ is added, $\mu(SCH_3)_2\mu(FCCF_3)Fe_2(CO)_4(P(CH_3)_3)_2$ (**5**) and $(\mu(SCH_3)Fe(CO)_2P(CH_3)_3)_2$ are obtained. The instability of **3** prevents further characterization, although a chemical analysis of the fresh precipitate agrees satisfactorily with the formulation $((\mu(SCH_3)Fe(CO)_2)_3(C_2F_4))_n$.

The fluorine migration which leads from **1** to **2** is a well-established reaction, as it occurs, for instance, in the reaction of nucleophilic carbonyl metal anions with perfluoroallyl chloride[22] and in the reactions of hexafluorobuta-1,3-diene

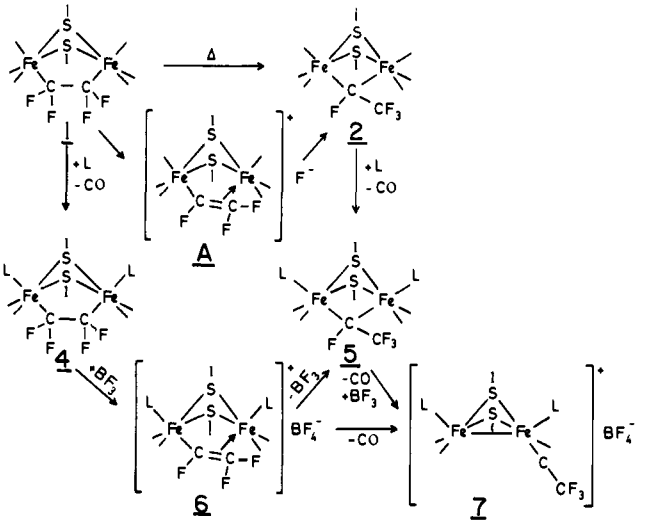

Figure 3. Overall summary of the proposed mechanism and identified products in the rearrangement of the C_2F_4 bridging group to the >CF-CF_3 bridge and to the C-CF_3 terminal carbyne group.

with hydridopentacarbonylmanganese.[23] The same type of rearrangement has also been observed in the reaction of hexafluoropropene with Pt(1,5-C_8H_{12})$_2$, for which a mechanism has been suggested.[21] A similar mechanism is proposed here (Figure 2). In the proposed intermediate compound A of Figure 2 there is a σ-π bonded vinyl group. We can consider the β-carbon atom of this group to be electrophilic, as it is, for instance, in $Os_3H(HC{=}CH_2)(CO)_{10}$.[24] Thus it seems reasonable that an attack of F^- on this carbon atom of the CF_2 group generates the carbene compound **2**. Attempts to isolate the proposed intermediate compound A of Figure 2 using $BF_3{\cdot}O(CH_3)_2$, a fluoride ion abstractor for metal perfluoroalkyl compounds,[25] failed when starting with compound **1**. But if $P(CH_3)_3$ is added, two CO groups being substituted, the expected parent compound $[\mu(SCH_3)_2Fe_2(CO)_4(P(CH_3)_3)_2(FCCF_2)][BF_4]$ (**6**) is obtained. When starting with $\mu(SCH_3)_2\mu(C_2F_4)Fe_2(CO)_4P(CH_3)_3)_2$ (**4**), compound **6** is obtained in better yield. As for compound **4**, compound **6** shows three infrared-active bands in the ν(CO) stretching region but these are shifted to higher frequencies and a new, strong band at 1600 cm^{-1} appears which is in the region of the ν(C=C) stretching frequency of a coordinated fluoro olefin.[26] Another strong band at 1030 cm^{-1} is characteristic of BF_4^-. This result strongly suggests that **6** has structure A of Figure 2. Furthermore, this structure is consistent with the ^1H NMR spectrum, which shows the two phosphine ligands to be chemically different. Unfortunately the low solubility of **6** together with its low stability at room temperature did not allow us to obtain its ^{19}F NMR spectrum.

When a solution of **6** in dichloromethane is left at room temperature, the color rapidly changes from violet to deep red and 1 mol of CO gas is evolved per mol of **6**. Infrared spectra in the ν(CO) stretching region show that a new compound **7** has been formed which exhibits three infrared-active ν(CO) bands at slightly lower frequencies and with different relative intensities than **6**. The ^{19}F NMR spectrum shows a single resonance at 78.4 ppm. Furthermore compound **7** is obtained when **5** is reacted with 1 equiv of $BF_3{\cdot}O(CH_3)_2$. Compound **7** analyzes as $[Fe_2(SCH_3)_2(CO)_3(P(CH_3)_3)_2(CCF_3)][BF_4]$. As the ^1H NMR spectrum of **7** shows that the phosphine ligands are chemically different, we propose a structure for **7** in which the C-CF_3 group is a terminal carbyne ligand and in which there is an Fe-Fe bond. Such a compound would appear to be the first example of a perfluoroalkylcarbyne complex. At this point, a question remains unanswered: how does **6** rearrange to give **7**? The most probable route seems to be the abstraction of F^- from BF_4^- giving compound **5** which is then attacked by the liberated BF_3 to give compound **7** after CO evolution. These proposed reactions are sketched in Figure 3.

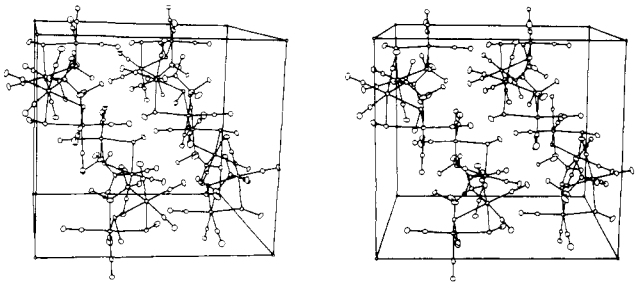

Figure 4. Stereoscopic view of a unit cell of $\mu(SCH_3)_2\mu(C_2F_4)Fe_2(CO)_6$. The x axis is horizontal from left to right, the y axis is perpendicular from bottom to top, and the z axis comes out of the paper. The vibrational ellipsoids are drawn at the 30% level. Hydrogen atoms are omitted. Disorder of the fluorine atoms is not shown.

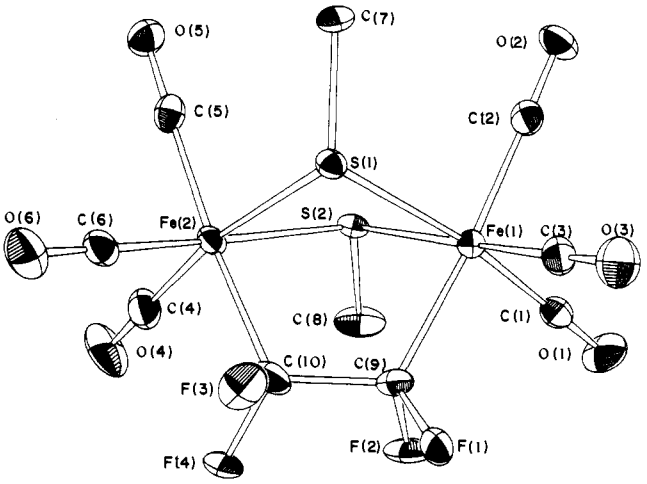

Figure 5. A perspective representation of a molecule of $\mu(SCH_3)_2\mu(C_2F_4)Fe_2(CO)_6$. The vibrational ellipsoids are drawn at 50% probability level. The labeling scheme is also shown.

Description of the Structures of 1 and 2. The crystal structure of **1** consists of the packing of eight dinuclear molecules. A stereoscopic packing diagram of the unit cell is shown in Figure 4. Bond distances and bond angles are given in Tables VI and VII, respectively. Figure 5 shows a perspective view of molecule **1** which includes the labeling scheme, while the stereoscopic view in Figure 6 depicts the disorder of the fluorine atoms. Table VIII[20] presents information on least-squares planes. The dinuclear molecule has roughly a mirror plane containing the two sulfur bridging atoms and the midpoint between the two iron atoms. Each iron atom is octahedrally coordinated to two bridging sulfur atoms of the methylthiolato groups, three carbon atoms of the carbon groups, and one carbon atom of the C_2F_4 group. The "flap" angle, the dihedral angle between the two planes containing S(1), S(2), and the equatorial carbon atoms of the carbonyl groups, is 135.0° (Table VIII), the separation of the two iron atoms is 3.311 (1) Å, and the mean Fe(1)-S-Fe(2) angle is 91.6 (1)°. These values show clearly that the dinuclear unit is opened around the S-S axis compared with the $(\mu(SC_2H_5)Fe(CO)_3)_2$ complex.[27] The C_2F_4 group bridges the two iron atoms through two σ(C-Fe) bonds (C(9)-Fe(1) and C(10)-Fe(2)), so that the C(9)-C(10) bond is parallel to the Fe(1)-Fe(2) direction. The C(9)-C(10) bond distance of 1.534 (7) Å is typical for a single bond. The methyl groups have their expected staggered con-

Table VI. Selected Distances (Å) in $\mu(SCH_3)_2\mu(C_2F_4)Fe_2(CO)_6$ (**1**)

	Fe–Fe	
Fe(1)–Fe(2)	3.311(1)	
	Fe–S	
Fe(1)–S(1)	2.312(2)	2.310(3)[a]
Fe(1)–S(2)	2.310(2)	
Fe(2)–S(1)	2.306(2)	
Fe(2)–S(2)	2.310(2)	
	Fe–C(equatorial)	
Fe(1)–C(1)	1.802(6)	1.801(5)
Fe(1)–C(3)	1.802(5)	
Fe(2)–C(4)	1.799(5)	
Fe(2)–C(6)	1.801(6)	
	Fe–C(axial)	
Fe(1)–C(2)	1.859(6)	1.859(6)
Fe(2)–C(5)	1.858(5)	
	Fe–C(C_2F_4)	
Fe(1)–C(9)	2.033(5)	2.024(11)
Fe(2)–C(10)	2.016(5)	
	C–C(C_2F_4)	
C(9)–C(10)	1.534(7)	
	S–C	
S(1)–C(7)	1.816(5)	1.821(8)
S(2)–C(8)	1.827(5)	
	C–F	
C(9)–F(1)	1.357(9)	
C(9)–F(2)	1.444(9)	
C(9)–F(1)′	1.430(11)	
C(9)–F(2)′	1.362(9)	
C(10)–F(3)	1.552(9)	1.41(13)
C(10)–F(4)	1.300(8)	
C(10)–F(3)′	1.241(9)	
C(10)–F(4)′	1.617(10)	
	C≡O	
C(1)–O(1)	1.132(6)	1.132(7)
C(2)–O(2)	1.127(6)	
C(3)–O(3)	1.142(6)	
C(4)–O(4)	1.127(6)	
C(5)–O(5)	1.126(6)	
C(6)–O(6)	1.139(6)	

[a] Here and in subsequent distance and angle tables the number in parentheses following a mean value is the larger standard deviation of a single observation as estimated from the inverse matrix or from the individual values on the assumption that they are from the same population.

figuration with respect to the S–Fe bonds, as shown by the values for the H–C–S–Fe torsion angles (Table IX).[20]

Model building of the dinuclear molecule of **1** shows that the two alternative positions for the fluorine atoms of the bridging C_2F_4 group can be reached with only a slight deformation of the S(1)–Fe(1)–C(9)–C(10)–Fe(2)–S(2) ring, i.e., with slight shifts of the C(9) and C(10) carbon atoms. This observation explains why the disorder of the fluorine atoms has satisfactorily been resolved without taking account of alternative positions for the two carbon atoms C(9) and C(10) to which they are attached; the anisotropic thermal motion of the carbon atoms is sufficient to handle this. However, the eight C–F bond distances vary from 1.357 (9) to 1.444 (9) Å around atom C(9) and from 1.240 (9) to 1.617 (10) Å around atom C(10). These variations are likely a manifestation of the disorder.

The crystal structure of **2** consists of the packing of eight dinuclear molecules. There are two independent dinuclear molecules, which we denote A and B, in the asymmetric unit.

Table VII. Selected Angles (deg) in $\mu(SCH_3)_2\mu(C_2F_4)Fe_2(CO)_6$ (**1**)

	S–Fe–S	
S(1)–Fe(1)–S(2)	80.49(5)	
	S–Fe–C(trans-equatorial)	
S(1)–Fe(1)–C(1)	171.6(2)	171.5(7)
S(2)–Fe(1)–C(3)	171.7(2)	
S(1)–Fe(2)–C(4)	170.4(2)	
S(2)–Fe(2)–C(6)	172.1(2)	
	S(1)–Fe–C(cis-equatorial)	
S(1)–Fe(1)–C(3)	91.4(2)	91.5(2)
S(1)–Fe(2)–C(6)	91.6(2)	
	S(2)–Fe–C(cis-equatorial)	
S(2)–Fe(1)–C(1)	93.7(2)	93.4(2)
S(2)–Fe(2)–C(4)	93.1(2)	
	S(1)–Fe–C(axial)	
S(1)–Fe(1)–C(2)	93.6(2)	93.5(2)
S(1)–Fe(2)–C(5)	93.4(2)	
	S(2)–Fe–C(axial)	
S(2)–Fe(1)–C(2)	88.8(2)	88.6(2)
S(2)–Fe(1)–C(5)	88.4(2)	
	S–Fe–C(C_2F_4)	
S(1)–Fe(1)–C(9)	83.2(2)	
S(2)–Fe(1)–C(9)	87.3(2)	
S(1)–Fe(2)–C(10)	82.0(2)	
S(2)–Fe(2)–C(10)	88.8(2)	
	Fe–S–Fe	
Fe(1)–S(1)–Fe(2)	91.64(5)	91.61(5)
Fe(1)–S(2)–Fe(2)	91.58(5)	
	Fe–S(1)–C(7)	
Fe(1)–S(1)–C(7)	107.8(1)	107.6(2)
Fe(2)–S(1)–C(7)	107.5(2)	
	Fe–S(2)–C(8)	
Fe(1)–S(2)–C(8)	113.3(2)	113.2(2)
Fe(2)–S(2)–C(8)	113.1(2)	
	Fe–C–F	
Fe(1)–C(9)–F(1)	116.5(5)	111.9
Fe(1)–C(9)–F(2)	109.4(4)	
Fe(1)–C(9)–F(1)′	107.1(5)	
Fe(1)–C(9)–F(2)′	114.0(5)	
Fe(2)–C(10)–F(3)	105.3(4)	
Fe(2)–C(10)–F(4)	117.5(5)	
Fe(2)–C(10)–F(3)′	120.8(5)	
Fe(2)–C(10)–F(4)′	104.2(4)	
	Fe—C≡O	
Fe(1)–C(1)–O(1)	178.1(5)	178.4(5)
Fe(1)–C(2)–O(2)	178.8(5)	
Fe(1)–C(3)–O(3)	178.3(5)	
Fe(2)–C(4)–O(4)	178.5(5)	
Fe(2)–C(5)–O(5)	178.4(5)	
Fe(2)–C(6)–O(6)	178.1(5)	
	C–C–F	
C(10)–C(9)–F(1)	114.1(5)	106
C(10)–C(9)–F(2)	97.1(5)	
C(10)–C(9)–F(1)′	97.8(6)	
C(10)–C(9)–F(2)′	118.6(6)	
C(9)–C(10)–F(3)	97.4(5)	
C(9)–C(10)–F(4)	117.0(5)	
C(9)–C(10)–F(3)′	116.1(6)	
C(9)–C(10)–F(4)′	93.3(7)	
	F–C–F	
F(1)–C(9)–F(2)	100.9(5)	99
F(1)′–C(9)–F(2)′	100.0(6)	
F(3)–C(10)–F(4)	97.8(6)	
F(3)′–C(10)–F(4)′	98.2(7)	

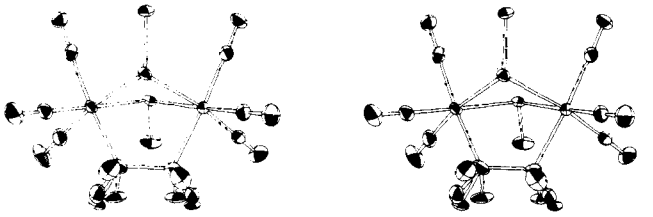

Figure 6. A stereoscopic view of a molecule of $\mu(SCH_3)_2\mu(C_2F_4)Fe_2(CO)_6$ showing the disorder of the fluorine atoms. The vibrational ellipsoids are drawn at 50% probability level. Hydrogen atoms are omitted.

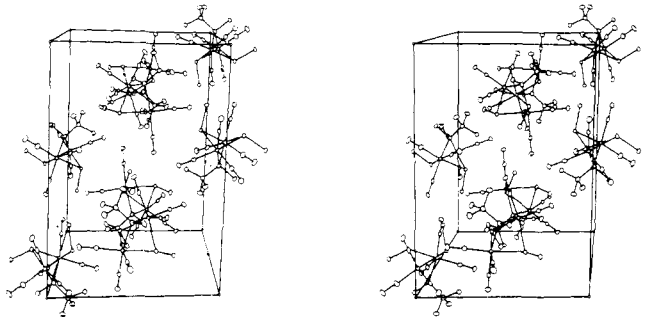

Figure 7. Stereoscopic view of a unit cell of $\mu(SCH_3)_2\mu(FCCF_3)Fe_2(CO)_6$. The x axis is perpendicular, the y axis goes from right to left, and the z axis comes out of the paper. The vibrational ellipsoids are drawn at the 30% probability level. Hydrogen atoms are omitted.

A stereoscopic packing diagram of the unit cell is shown in Figure 7. Bond distances, bond angles, and least-squares planes are listed in Tables X, XI, and XII,[20] respectively. Figure 8 shows a perspective view of one molecule of compound **2**. The dinuclear molecule has roughly a mirror plane which contains atoms S(1), S(2), and C(9) (see Table XII). Each iron atom is octahedrally coordinated to two bridging sulfur atoms of the methylthiolato groups, three carbon atoms of the carbonyl groups, and the bridging carbon atom of the $CF-CF_3$ group. The "flap" angle between the two planes containing S(1), S(2), and the equatorial carbon atoms of carbonyl groups averages 107.6 (5)° (Table XII). The mean value for the separation of the two iron atoms is 2.963 (6) Å and the mean Fe(1)-S-Fe(2) angle is 79.4 (2)°. The Fe_2S_2 core is thus more compact than in **1** but less than in $(\mu(SC_2H_5)Fe(CO)_3)_2$. The $CF-CF_3$ group behaves as a bridging carbene, the fluorine atoms of the trifluoromethyl portion being in a staggered position with respect to the C(9)-F(1) bond in both molecules A and B, as can be seen in Figure 8 or from F(i)-C(10)-C(9)-F(1) (i = 2, 3, or 4) torsion angles given in Table XIII.[20] The average Fe-C bond of 2.037 Å in **2** is in the expected range[27,28] for a carbene group bridging two metal atoms. The two methyl groups occupy positions which give an anti configuration for both molecules A and B. For the methyl group in the endo position, in both molecules A and B the hydrogen atoms are eclipsed with respect to the S-Fe bonds (see Table XIII for H-C-S-Fe torsion angles). For the methyl group in the exo position, the hydrogen atoms are in the staggered configuration in molecule A and in the eclipsed configuration in molecule B with respect to the S-Fe bonds. This difference in the configuration of the H atoms on the exo methyl group is the major one between molecules A and B.

The average Fe-C(carbonyl) distance trans to any bridging sulfur atom (1.801 Å for **1**, 1.790 Å for **2**) lies within the expected range.[29-33] The Fe-C axial carbonyl distance, however, is significantly longer (1.859 (6) Å for **1**, 1.848 (5) Å for **2**) suggesting facile CO abstraction which is consistent with the formation of the green product **3**.

The Fe_2S_2 core varies considerably from compound **1** to compound **2** and is compared with those observed in various $(\mu(SR)Fe(CO)_3)_2$ complexes[29-31] in Table XIV. As pointed out earlier,[34] different substituents on the sulfur bridging atom

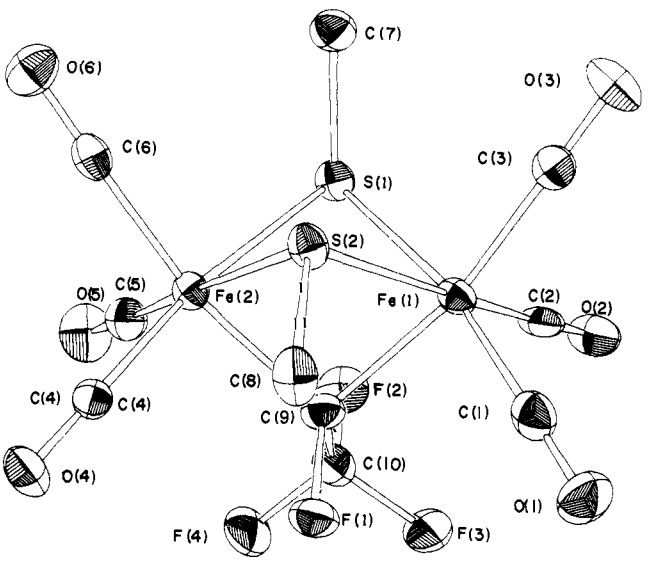

Figure 8. A perspective representation of one of the two independent molecules of $\mu(SCH_3)_2\mu(FCCF_3)Fe_2(CO)_6$.

Table X. Selected Distances (Å) in $\mu(SCH_3)_2\mu(FCCF_3)Fe_2(CO)_6$ (**2**)

	molecule A	molecule B	av values
	Fe-Fe		
Fe(1)-Fe(2)	2.958(1)	2.969(1)	2.963(6)
	Fe-S		
Fe(1)-S(1)	2.316(1)	2.321(2)	2.320(4)
Fe(1)-S(2)	2.314(1)	2.323(1)	
Fe(2)-S(1)	2.319(1)	2.316(1)	
Fe(2)-S(2)	2.323(1)	2.326(1)	
	Fe-C(equatorial)		
Fe(1)-C(1)	1.785(5)	1.787(5)	1.790(7)
Fe(1)-C(2)	1.791(5)	1.784(5)	
Fe(2)-C(4)	1.805(5)	1.788(5)	
Fe(2)-C(5)	1.786(5)	1.793(5)	
	Fe-C(axial)		
Fe(1)-C(3)	1.855(5)	1.842(5)	1.848(5)
Fe(2)-C(6)	1.849(5)	1.848(5)	
	Fe-C(carbene)		
Fe(1)-C(9)	2.028(5)	2.048(5)	2.037(7)
Fe(2)-C(9)	2.036(5)	2.035(5)	
	C-C		
C(9)-C(10)	1.487(7)	1.488(7)	1.488(7)
	C(9)-F		
C(9)-F(1)	1.444(5)	1.436(5)	1.440(5)
	CF_3		
C(10)-F(2)	1.336(5)	1.344(6)	1.354(14)
C(10)-F(3)	1.358(5)	1.374(6)	
C(10)-F(4)	1.364(6)	1.347(5)	
	S-C		
S(1)-C(7)	1.820(5)	1.810(5)	1.816(6)
S(2)-C(8)	1.812(4)	1.821(4)	
	C=O		
C(1)-O(1)	1.137(5)	1.140(6)	1.137(6)
C(2)-O(2)	1.143(5)	1.143(5)	
C(3)-O(3)	1.130(5)	1.135(5)	
C(4)-O(4)	1.127(5)	1.138(5)	
C(5)-O(5)	1.139(5)	1.143(6)	
C(6)-O(6)	1.131(5)	1.132(5)	

Table XI. Selected Bond Angles (deg) in $\mu(SCH_3)_2\mu(FCCF_3)Fe_2(CO)_6$

	molecule A	molecule B	av values
	S-Fe-S		
S(1)-Fe(1)-S(2)	81.62(5)	81.49(4)	81.50(11)
S(1)-Fe(2)-S(2)	81.36(5)	81.53(4)	
	S-Fe-C(trans equatorial carbonyl)		
S(1)-Fe(1)-C(1)	168.3(1)	168.5(2)	170.2(1.5)
S(2)-Fe(1)-C(2)	170.6(1)	171.7(2)	
S(1)-Fe(2)-C(4)	169.6(2)	169.6(1)	
S(2)-Fe(2)-C(5)	170.2(1)	173.1(1)	
	S-Fe-C(cis equatorial carbonyl)		
S(1)-Fe(1)-C(2)	89.1(1)	90.4(2)	92.0(2.1)
S(2)-Fe(1)-C(1)	94.0(1)	94.8(1)	
S(1)-Fe(2)-C(5)	89.6(1)	92.3(1)	
S(2)-Fe(2)-C(4)	93.9(2)	91.6(1)	
	S-Fe-C(axial carbonyl)		
S(1)-Fe(1)-C(3)	95.1(1)	94.1(1)	91.5(2.6)
S(2)-Fe(1)-C(3)	88.0(1)	89.4(1)	
S(1)-Fe(2)-C(6)	93.0(1)	91.9(1)	
S(2)-Fe(2)-C(6)	88.8(1)	91.9(1)	
	S-Fe-C(carbene)		
S(1)-Fe(1)-C(9)	79.2(1)	78.5(1)	79.4(6)
S(2)-Fe(1)-C(9)	79.9(1)	79.8(1)	
S(1)-Fe(2)-C(9)	79.0(1)	78.9(1)	
S(2)-Fe(2)-C(9)	79.5(1)	80.0(1)	
	Fe-S-Fe		
Fe(1)-S(1)-Fe(2)	79.31(4)	79.61(4)	79.4(2)
Fe(1)-S(2)-Fe(2)	79.25(4)	79.37(4)	
	Fe-S-CH_3(exo)		
Fe(1)-S(1)-C(7)	108.5(2)	108.8(2)	109.0(5)
Fe(2)-S(1)-C(7)	109.4(2)	109.3(2)	
	Fe-S-CH_3(endo)		
Fe(1)-S(2)-C(8)	113.4(2)	111.0(2)	112.4(1.1)
Fe(2)-S(2)-C(8)	111.7(2)	112.2(2)	
	Fe-C-Fe		
Fe(1)-C(9)-Fe(2)	93.4(1)	93.3(1)	93.4(1)
	Fe-C-F		
Fe(1)-C(9)-F(1)	113.1(3)	111.9(3)	112.4(7)
Fe(2)-C(9)-F(1)	111.6(3)	112.9(3)	
	Fe-C-C		
Fe(1)-C(9)-C(10)	118.4(3)	118.3(3)	119.4(1.2)
Fe(2)-C(9)-C(10)	120.7(3)	120.0(3)	
	Fe-C≡O		
Fe(1)-C(1)-O(1)	178.3(4)	178.6(5)	178.0(9)
Fe(1)-C(2)-O(2)	178.2(4)	177.8(5)	
Fe(1)-C(3)-O(3)	176.5(4)	178.7(4)	
Fe(2)-C(4)-O(4)	178.6(4)	178.2(4)	
Fe(2)-C(5)-O(5)	179.7(4)	177.5(4)	
Fe(2)-C(6)-O(6)	177.0(4)	177.2(4)	
	F-C-C		
F(1)-C(9)-C(10)	100.3(4)	101.1(3)	100.7(6)
	F-C-CF_3		
C(9)-C(10)-F(2)	112.8(4)	112.8(4)	112.5(5)
C(9)-C(10)-F(3)	112.1(4)	111.9(4)	
C(9)-C(10)-F(4)	112.2(4)	113.3(4)	
	F-C-F of CF_3		
F(2)-C(10)-F(3)	106.5(4)	106.0(4)	106.2(6)
F(2)-C(10)-F(4)	107.0(4)	106.8(4)	
F(3)-C(10)-F(4)	105.7(4)	105.4(4)	

Table XIV. Comparison of Selected Average Values of Distances (Å) and Angles (deg) in $\mu(SCH_3)\mu(C_2F_4)Fe_2(CO)_6$ (**1**) and $\mu(SCH_3)\mu(FCCF_3)Fe_2(CO)_6$ (**2**) with Those in $\mu(SR)Fe(CO)_3)_2$ Compounds

	1	2	range for $(\mu(SR)$-$Fe(CO)_3)_2$[a]
	Distances		
Fe(1)-Fe(2)	3.311(1)	2.963(6)	2.507-2.540
Fe-S	2.310(3)	2.320(4)	2.248-2.281
Fe-C(equatorial)	1.801(5)	1.790(7)	1.772-1.810
Fe-C(axial)	1.859(6)	1.848(5)	
S-S	2.986(2)	3.029(7)	2.817-2.932
	Angles		
Fe-S-Fe	91.61(5)	79.4(6)	67.0-68.8
S-Fe-C(trans)	171.5(7)	170.2(1.5)	
S-Fe-C(cis)	91.5-93.4	92.0(2.1)	
S-Fe-C(axial)	88.6-93.5	91.5(2.6)	
flap angle	135.0	107.6	87.9-95.2

of thiolate groups produce only small differences in the geometry of the central Fe_2S_2 core: the ranges are reported in Table XIV. This relatively constant geometry can be considered typical when the bridging atoms are sulfur and when the bent Fe-Fe bond is present. This geometry is only slightly affected when these complexes are protonated to yield hydrido-bridged species.[33] But, as expected, there is a considerable change in Fe_2S_2 geometry when a carbene (compound **2**) or C_2 (compound **1**) bridge is formed. Major changes occur in the "flap" angle, the Fe-S-Fe angle, and the Fe-Fe distance, while the Fe-S distances are only slightly affected (Table XIV). The changes naturally are larger for compound **1** than for compound **2**.

Acknowledgments. J.J.B. wishes to acknowledge the receipt of a NSF-CNRS Exchange Fellowship, which has made his leave from the University of Toulouse possible. This work was supported in part at Northwestern University by the National Science Foundation (Grant CHE76-10335).

Supplementary Material Available: Tables of observed and calculated structure amplitudes for compounds **1** and **2**, root-mean-square amplitudes of vibration (Tables III and V), least-squares planes (Tables VIII and XII), and torsion angles (Tables IX and XIII) (36 pages). Ordering information is given on any current masthead page.

References and Notes

(1) (a) Laboratoire de Chimie de Coordination. (b) Northwestern University.
(2) (a) Bailey, Jr., W. I.; Chisholm, M. H.; Cotton, F. A.; Murillo, C. A.; Rankel, L. A. *J. Am. Chem. Soc.* **1978**, *100*, 802-806. (b) Chisholm, M. H.; Cotton, F. A.; Extine, M. W.; Rankel, L. A. *Ibid.* **1978**, *100*, 807-811.
(3) Chisholm, M. H.; Cotton, F. A.; Extine, M. W.; Kelly, R. L. *J. Am. Chem. Soc.* **1978**, *100*, 3354-3358.
(4) Davidson, J. L.; Sharp, D. W. A. *J. Chem. Soc., Dalton Trans.* **1975**, 2283-2287.
(5) Hoehn, H. H.; Pratt, L.; Watterson, K. F.; Wilkinson, G. *J. Chem. Soc.* **1961**, 2738-2745.
(6) Booth, B. L.; Haszeldine, R. N.; Mitchell, P. R.; Cox, J. J. *Chem. Commun.* **1967**, 529-530.
(7) Fischer, E. O.; Maasböl, A. *Angew. Chem.* **1964**, *76*, 645.
(8) Huttner, G.; Regler, D. *Chem. Ber.* **1972**, *105*, 2726.
(9) Yamamoto, T.; Garber, A.R.; Wilkinson, J. R.; Boss, C. B.; Streib, W. E.; Todd, L. J. *J. Chem. Soc., Chem. Commun.* **1974**, 354-356.
(10) Aumann, R.; Wormann, H.; Krugger, C. *Angew. Chem., Int. Ed. Engl.* **1976**, *15*, 609-610.
(11) Cook, P. M.; Dahl, L. F.; Dickerhoof, D. W. *J. Am. Chem. Soc.* **1972**, *94*, 5511-5513.
(12) Herrmann, W. A. *Angew. Chem., Int. Ed. Engl.* **1978**, *17*, 800-812, and references cited therein.
(13) Mathieu, R.; Poilblanc, R. *J. Organomet. Chem.* **1977**, *142*, 351-355.
(14) Corfield, P. W. R.; Doedens, R. J.; Ibers, J. A. *Inorg. Chem.* **1967**, *6*, 197-204. Doedens, R. J.; Ibers, J. A. *Ibid.* **1967**, *6*, 204-210.
(15) See, for example, Waters, J. M.; Ibers, J. A. *Inorg. Chem.* **1977**, *16*, 3273-3277.
(16) The Northwestern absorption program, AGNOST, includes both the Coppens-Leiserowitz-Rabinovich logic for Gaussian integration and the

Tompa-De Meulenaur analytical method. In addition to various local programs for the CDC 6600 computer, modified versions of the following were employed: MULTAN, direct method program of Main, Germain, and Woolfson, Zalkin's FORDAP Fourier summation program, Johnson's ORTEP thermal ellipsoid plotting program, and Busing's and Levy's ORFFE error function program. Our full-matrix least-squares program, NUCLS, in its nongroup form, closely resembles the Busing-Levy ORFLS program.
(17) Cromer, D. T.; Waber, J. T. "International Tables for X-ray Crystallography", Vol. IV; Kynoch Press: Birmingham, England, 1974; Table 2.2A. Cromer, D. T. *Ibid.*, Table 2.3.1.
(18) Stewart, R. F.; Davidson, E. R.; Simpson, W. T. *J. Chem. Phys.* **1965**, *42*, 3175-3179.
(19) Ibers, J. A.; Hamilton, W. C. *Acta Crystallogr.* **1964**, *17*, 781-782.
(20) See paragraph at end of paper regarding supplementary material.
(21) Green, M.; Laguna, A.; Spencer, J. L.; Stone, F. G. A. *J. Chem. Soc., Dalton Trans.* **1977**, 1010-1016.
(22) McClellan, W. R. *J. Am. Chem. Soc.* **1961**, *83*, 1598-1601.
(23) Tattershall, B. W.; Rest, A. J.; Green, M.; Stone, F. G. A. *J. Chem. Soc.* **1968**, 899-902.
(24) Churchill, M. R.; DeBoer, B. G.; Shapley, J. R.; Keister, J. B. *J. Am. Chem. Soc.* **1976**, *98*, 2357-2358.
(25) Reger, D. L.; Dukes, M. D. *J. Organomet. Chem.* **1978**, *153*, 67-72.
(26) Fields, R.; Godwin, G. L.; Haszeldine, R. N. *J. Chem. Soc., Dalton Trans.* **1975**, 1867-1872.
(27) Huttner, G.; Gartzke, W. *Chem. Ber.* **1972**, *105*, 2714.
(28) Yamamoto, Y.; Aoki, K.; Yamazaki, H. *J. Am. Chem. Soc.* **1974**, *96*, 2647-2648.
(29) Dahl, L. F.; Wei, C. H. *Inorg. Chem.* **1963**, *2*, 328-333.
(30) Henslee, W.; Davis, R. E. *Cryst. Struct. Commun.* **1972**, *403*, 185.
(31) Coleman, J. M.; Wojcicki, A.; Pollick, P. J.; Dahl, L. F. *Inorg. Chem.* **1967**, *6*, 1236-1242.
(32) Le Borgne, G.; Grandjean, D.; Mathieu, R.; Poilblanc, R. *J. Organomet. Chem.* **1977**, *131*, 429-438.
(33) Savariault, J. M.; Bonnet, J. J.; Mathieu, R.; Galy, J. *C. R. Acad. Sci., Ser. C* **1977**, *284*, 663-665.
(34) Clegg, W. *Inorg. Chem.* **1976**, *15*, 1609-1613.

Structure of η^3-Cyclooctenyltris(trimethyl phosphite)iron(I). Bonding of the η^3-Alkenyl Group to 16-, 17-, and 18-Electron ML_3 Systems

R. L. Harlow, R. J. McKinney, and S. D. Ittel*

Contribution No. 2673 from the Central Research and Development Department, E. I. du Pont de Nemours and Company, Experimental Station, Wilmington, Delaware 19898. *Received June 13, 1979*

Abstract: The crystal and molecular structure of $Fe(\eta^3\text{-}C_8H_{13})(P(OMe)_3)_3$ has been determined at −80 °C by X-ray diffraction. The monoclinic crystals ($C2/c$) have unit cell dimensions a = 14.940 (3) Å, b = 11.626 (3) Å, c = 29.952 (5) Å, β = 103.88 (2)°, and V = 5050.5 Å^3. Full-matrix least-squares refinement led to $R(F_o)$ = 0.035 and $R_w(F_o)$ = 0.036. The coordination sphere about the iron atom is a distorted square pyramid if the η^3-cyclooctenyl group is considered to be a bidentate ligand. The η^3-allylic group is symmetrical but skewed with respect to the basal plane. This twisting allows a hydrogen atom on a carbon atom attached to the η^3-allylic group to have a very weak (2.77 (2) Å) interaction with the metal center. Extended Hückel theory, with the inclusion of two-body repulsion, has been used to reproduce molecular geometries, including bond lengths, of 16-, 17-, and 18-electron complexes of the type $[M(\eta^3\text{-alkenyl})(P(OMe)_3]^{+x}$. Barriers to several intramolecular rearrangements have been calculated for these species and agree well with NMR and ESR measurements. The bonding in the 16-, 17-, and 18-electron species is discussed.

Introduction

The dimeric species, $[Fe(\eta^3\text{-allyl})(CO)_3]_2$, prepared by a

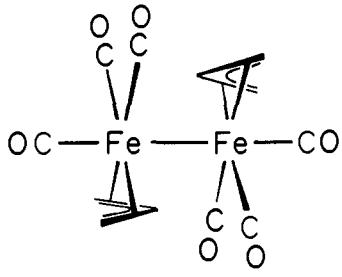

one-electron reduction of $FeX(\eta^3\text{-allyl})(CO)_3$ complexes (where X = halide), has been shown to exist in equilibrium with its paramagnetic monomer.[1-3] This monomer-dimer equilibrium is very sensitive to steric effects. Thus, if substituents are added to the allyl group,[1] or one or more of the carbonyl ligands are replaced with phosphorus ligands,[1,2] the equilibrium is shifted dramatically toward the monomeric species.

The phosphite complex $[Fe(\eta^3\text{-cyclooctenyl})(P(OMe)_3)_3][BF_4]$[4,5] (**1**) undergoes a similar one-electron reduction to give the monomeric species $Fe(\eta^3\text{-cyclooctenyl})(P(OMe)_3)_3$[6] (**2**). Complex **2** shows no tendency to form a

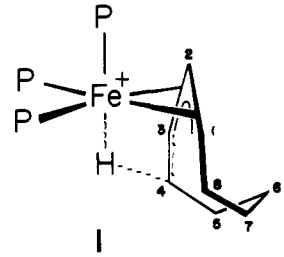

I

diamagnetic dimer. Additionally, it is fluxional on the ESR time scale, showing hyperfine coupling to three nonequivalent[7] phosphorus nuclei in slow exchange at −140 °C. As the system is warmed a dynamic process begins to equilibrate the two similar phosphorus nuclei until at −60 °C the spectrum appears as a doublet of triplets. As the system is warmed further, a second, independent fluxional process begins to equilibrate all three phosphorus nuclei, giving a quartet at 140 °C. While we were able to simulate the permutational behavior of the phosphorus nuclei, without some knowledge of the ground-state geometry, we were unable to draw any conclusions about the physical dynamic process related to that permutational behavior.

The crystal structure of the dimeric species $[Fe(\eta^3\text{-}C_3H_5)(CO)_3]_2$ has been reported,[3] but from spectroscopic measurements the solution structure of **2** is clearly of lower symmetry than would be expected for half of the dimer. Two

0002-7863/79/1501-7496$01.00/0